Corepressor-Dependent Silencing of Chromosomal Regions Encoding Neuronal Genes

Victoria V. Lunyak,[1] Robert Burgess,[1]* Gratien G. Prefontaine,[1] Charles Nelson,[1] Sing-Hoi Sze,[2] Josh Chenoweth,[3] Phillip Schwartz,[4] Pavel A. Pevzner,[2] Christopher Glass,[5] Gail Mandel,[3] Michael G. Rosenfeld[1]†

The molecular mechanisms by which central nervous system–specific genes are expressed only in the nervous system and repressed in other tissues remain a central issue in developmental and regulatory biology. Here, we report that the zinc-finger gene-specific repressor element RE-1 silencing transcription factor/neuronal restricted silencing factor (REST/NRSF) can mediate extraneuronal restriction by imposing either active repression via histone deacetylase recruitment or long-term gene silencing using a distinct functional complex. Silencing of neuronal-specific genes requires the recruitment of an associated corepressor, CoREST, that serves as a functional molecular beacon for the recruitment of molecular machinery that imposes silencing across a chromosomal interval, including transcriptional units that do not themselves contain REST/NRSF response elements.

Specific strategies mediating gene repression and gene silencing are required to generate cell-type diversity and promote inheritable cell-type identity [reviewed in (*1*)]. For example, the transcriptional repression of neuronal-specific genes is necessary to maintain functions unique to nonneuronal systems. Although the precise mechanisms responsible for this tissue-specific transcriptional inactivation remain unclear, it has been shown that repressor element RE-1 silencing transcription factor/neuronal restricted silencing factor (REST/NRSF) is a negative regulator that restricts expression of neuronal genes to neurons in a variety of genetic contexts (*2–4*). About 35 neuronal target genes have been identified for REST/NRSF [reviewed in (*4*)]. REST/NRSF is a 116-kD protein that contains a DNA binding domain with eight zinc fingers and two repressor domains (*4–6*) and binds to a 21– to 23–base pair (bp) conserved DNA response element, RE-1/NRSE (*2–4*). It has been shown that REST/NRSF can mediate repression, in part, through the association of its NH_2-terminal repression domain with the mSin3/histone deacethylase 1,2 (HDAC1,2) complex and with the nuclear receptor corepressor (N-CoR) participating in the context of certain genes (*7*, *8*). The REST/NRSF COOH-terminal repression domain associates with at least one other factor, the transcriptional corepressor CoREST, characterized by two SWI3, ADA2, N-Cor, TFIIIB (SANT) domains (*9*), that may serve as a platform protein for assembly of specialized repressor machinery (*10–12*) (fig. S1).

HDAC-dependent repression of the neuron-specific gene *SCG10*. REST/NRSF alternatively recruits mSin3A/HDAC1,2 (*7*, *8*) or CoREST complexes (*10–12*). To investigate the molecular mechanisms involved in REST/NRSF-mediated gene repression and corepressor complexes, we studied one of the most well-characterized neuronal-specific genes, *NaCh type II/Nav1.2*, and compared its regulation to that of *SCG10* (*5–8*). In a chromatin immunoprecipitation assay (ChIP) (*8*, *13*) from Rat-1 fibroblasts, REST/NRSF and CoREST were highly recruited to the *NaCh II* promoter, whereas N-CoR was not (Fig. 1A). HDAC1, HDAC3, and HDAC2 were detected in small quantities or not at all in some experiments (*14*). In contrast, REST/NRSF was present on the *SCG10* gene promoter with HDAC2, HDAC3, and N-CoR (*6*, *8*, *14*). Transfection of a construct that encodes the REST/NRSF DNA binding domain ($REST_{DBD}$) harboring deletions of the defined NH_2- and COOH-terminal repressor domains (*6*, *13*), and hence a potential dominant negative, resulted in the specific derepression of both the *SCG10* and *NaCh II* genes (Fig. 1B). Thus, the binding of REST functions in both establishing and maintaining repression (*2–4*).

Overexpression of the REST/NRSF interaction domain of CoREST ($CoREST_{RID}$) (*6*) served as a dominant negative in the Rat-1 cells and resulted in the specific derepression of the *NaCh II* gene (Fig. 1C); in contrast, there was no effect on repression of the *SCG10* gene (Fig. 1C). Because CoREST can form a biochemical complex with HDAC1/2 (*10–12*), we investigated the functional importance of HDACs by treating Rat-1 cells with an HDAC inhibitor, trichostatin A (TSA) (300 nM) (*7*). When exponentially proliferating Rat-1 cells were incubated in the presence of 300 nM TSA, ectopic activation of the *SCG10* gene was observed, with the maximum level of expression activity 8 hours after treatment (Fig. 1D). In contrast, even after a 48-hour treatment with TSA no detectable activation of the *NaCh II* gene was observed (Fig. 1D). These data indicate that CoREST is selectively required to maintain *NaCh II* but not *SCG10* gene repression.

CpG methylation is required for silencing *NaCh II* gene transcription. Because TSA failed to reduce *NaCh II* gene repression and because DNA methylation is a widely used strategy in gene silencing (*15*), we examined the CpG methylation status of the *NaCh II* gene in Rat-1 cells. Within the genome, from 60 to 90% of the cytosine methylation occurs at CpG dinucleotides (*15–17*). With the use of the sodium bisulfite genomic-modification sequencing approach (*13*), we found that the *NaCh II* promoter region exhibited a sparse pattern of CpG methylation (C^mpG), with three sites (−447, −259, and +45) preferentially methylated, whereas the CpGs further along the 3′ end of the gene exhibited a more robust methylated CpG pattern (Fig. 1E) (*14*). Treatment of Rat-1 cells with 5′-aza-cytidine (5AzaC) for a prolonged period of time (up to 72 hours) to reverse DNA methylation reduced specific CpG methylation in the *NaCh II* gene promoter (Fig. 1F and fig. S2) and caused derepression of the *NaCh II* but not the *SCG-10* gene (Fig. 1G). These data suggest that the *NaCh II* gene might be silenced in a C^mpG-dependent manner.

Among the many proteins that bind to methylated DNA, MeCP2 characteristically binds to single, symmetrical C^mpG pairs in any sequence context (*18–20*) and has been functionally linked to gene silencing (*21–24*). Because it is also robustly expressed in Rat-1 cells (fig. S3), we investigated the possible participation of MeCP2 in *NaCh II* gene repression. ChIPs were performed from Rat-1 cells using a MeCP2-specific immunoglobulin G (IgG) (Fig. 2A) and primers from the REST-binding element in the promoters as well as from the 3′-coding regions of *SCG10* and *NaCh II* genes. MeCP2 is present in both the promoter and exon and intron regions of

[1]Howard Hughes Medical Institute (HHMI), [2]Department of Computer Science and Engineering, School of Medicine, University of California, San Diego, 9500 Gilman Drive, Room 345, La Jolla, CA 92093–0648, USA. [3]Howard Hughes Medical Institute, Department of Neurobiology, State University of New York, Stony Brook, NY 11794, USA. [4]Affinity BioReagents, Incorporated, 14818 West 6th Avenue, Suite 10A, Golden, CO 80401, USA. [5]Department of Cellular and Molecular Medicine, School of Medicine, University of California, San Diego, La Jolla, CA 92093, USA.

*Present address: Beckman Institute for Biomedical Research, Department of Functional Genomics, Temecula, CA 92590, USA.

†To whom correspondence should be addressed. E-mail: mrosenfeld@ucsd.edu

the *NaCh II* gene but does not bind to the *SCG10* gene (Fig. 2A). No detectable quantities of the methyl DNA binding proteins MBD3 or MBD4 were observed on the *NaCh II* gene promoter (*14*). In light of recent reports of a biochemical interactions between MeCP2 and transcriptional corepressors (*25*), we investigated the relationship between MeCP2 and CoREST. An affinity-purified polyclonal CoREST antibody (*6*) was used in immunoprecipitation assays (*13*) to detect direct or indirect interactions between endogenous MeCP2 and CoREST in Rat-1 cells (Fig. 2B). The overexpression of the DNA binding domain of MeCP2 ($MeCP2_{MDB}$) as a putative dominant negative resulted in derepression of the *NaCh II* gene, but had no effect on repression of the *SCG10* gene (Fig. 2C). The effects of $MeCP2_{MDB}$ on derepression of *NaCh II* gene transcription after >12 hours in synchronized Rat-1 cells suggest that it blocks reestablishment of the repression apparatus after DNA replication (Fig. 2D). Although the class I HDACs were shown to interact with MeCP2 via mSin3 (*18*), MeCP2 is preferentially localized to pericentromeric heterochromatin (*20*), a region of the highest 5′-C^mpG concentration (*21*), suggesting that some components of heterochromatic establishment may use MeCP2 as a readout for long-term repression. Our data, thus, indicate a requirement for MeCP2 as well as REST, CoREST, and DNA methylation in establishing and maintaining TSA-independent repression of the *NaCh II* gene in Rat-1 cells.

To determine whether the similar events that led to the formation of silenced regions at the centromere, at mating-type loci, and during X chromosome inactivation (*26–34*) pertain to REST/CoREST-dependent gene silencing, we applied ChIP analysis, which revealed the presence of heterochromatic protein 1 (HP1) as well as MeCP2 (Fig. 2E) and CoREST (Fig. 1A) on the *NaCh II* promoter. HP1 interacts with a specially modified histone H3 (dimethyl K^m9 histone H3) and is proposed to cause spreading of heterochromatic regions at the β-globin locus and in X chromosome inactivation (*25–27*). Indeed, dimethyl K^m9 histone H3 was observed on the *NaCh II* but not on the *SCG10* promoter (Fig. 2E).

Immunoprecipitation from Rat-1 cells of hemagglutinin (HA)–tagged holo-MeCP2 or HA-tagged $MeCP2_{DBD}$ revealed histone H3- but not histone H4-specific methyltransferase activity in the immunoprecipitated complex containing holo-MeCP2 (*34*) (Fig. 2F). In contrast, no methyltransferase activity was recovered from immunoprecipitated complexes associated with the HA-tagged dominant-negative form of MeCP2 ($MeCP2_{DBD}$) (Fig. 2F).

Mammalian histone lysine methyltransferase, suppressor of variegation 39H1 (SUV39H1), initiates silencing with selective methylation on Lys^9 of histone H3, thus creating a high-affinity binding site for HP1 (*34–36*). When an antibody to endogenous SUV39H1 was used for immunoprecipitation, MeCP2 was effectively coimmunoprecipitated; conversely, αHA antibodies to HA-tagged MeCP2 could immunoprecipitate SUV39H1 (Fig. 2G). Two consecutive rounds of immunoprecipitation for the ChIP showed that MeCP2 and SUV39H1 (Fig. 2H) and CoREST and MeCP2 (fig. S4) were present on the same *NaCh II* transcription units (Fig. 2I). Further, MeCP2 was selectively immunoprecipitated from mixed histones prepared from Rat-1 cell nuclei by αdi-Me K9 histone H3, but not αAcK14 histone H3 or αP10 H3 histone IgGs (*14*).

CoREST-dependent silencing of a chromosomal region. To identify previously unknown REST/NRSF target genes (*5*), we conducted a human and murine genome-wide search for REST/NRSF binding sites on the basis of the consensus site derived from experimentally confirmed RE1/NRSF with four invariant residues critical for function and

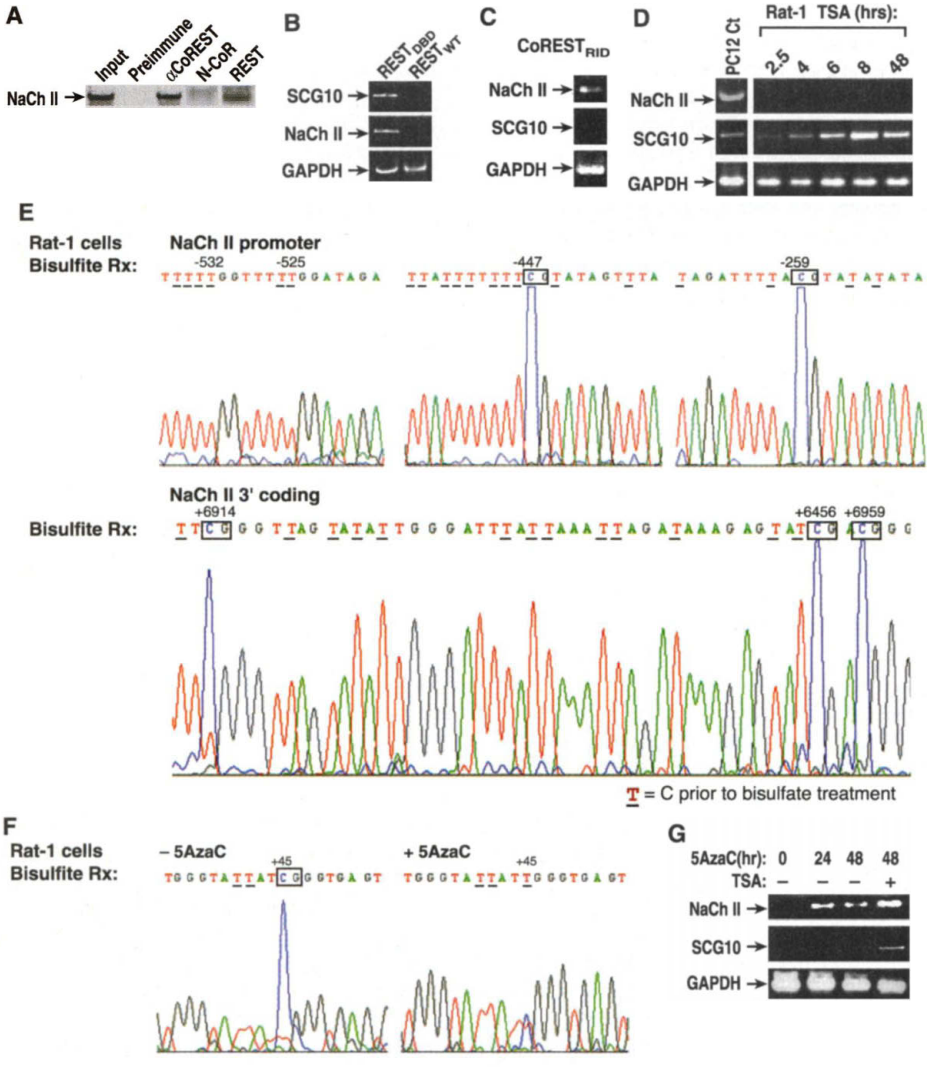

Fig. 1. REST/NRSF can mediate HDAC-dependent and DNA methylation–dependent repression of neuronal-specific genes in Rat-1 fibroblasts. (**A**) ChIP in Rat-1 fibroblasts, using PCR primers specific for the REST-containing regions in *NaCh II* and IgGs specific to CoREST, REST/NRSF, and N-CoR. (**B**) Analysis of *SCG10* and *NaCh II* transcripts with transient expression of $REST_{DBD}$ or $REST_{WT}$ in Rat-1 cells as detected by reverse transcriptase PCR (RT-PCR). PC12 cells and constitutively expressed glyceraldehyde-3-phosphate dehydrogenase (*GAPDH*) were used as controls. (**C**) *NaCh II* but not *SCG10* gene repression is reversed by transient expression of $CoREST_{RID}$. (**D**) Ectopic activation of the *SCG10* gene in TSA-treated (300 nM) Rat-1 fibroblasts. (**E**) Mapping of methylation status of *NaCh II* gene by bisulfite-modification sequencing in Rat-1 cells (*22*), in the promoter (upper) and further 3′ region within the *NaCh II* gene (lower). Methylated CpG pairs shown as open boxes, with unmethylated C converted to T (underlined) upon bisulfite treatment. (**F**) Change in DNA methylation status and (**G**) restoration of *NaCh II* gene expression after 5AzaC treatment in Rat-1 cells. Rat-1 cells treated with 10 μM of 5AzaC in the absence (–) or presence (+) of 300 nM of TSA. Total RNA was isolated for the detection of *NaCh II* or *SCG10* mRNA by RT-PCR.

permitting four mismatches (*13*, *37*). This bioinformatics approach revealed 1047 potential REST-binding sites in the genome, all but 40 located adjacent (±2 kb) to known or predicted genes.

Many of the putative REST/NRSF target genes have sufficiently well-characterized expression patterns, suggesting that ~90% can be assigned as strictly or predominantly neural-specific. The predicted genes encode a wide variety of functional molecules including ligands; ion channels; receptors; receptor-associated factors; and cytoskeletal and adhesion molecule–factors involved in axonal guidance, transport machinery, transcription factors, and cofactors; a portion of which are listed in Table 1. However, some genes are not neuronal-specific, including a cohort of genes involved in angiogenesis and chromatin remodeling. Evaluation of the effects of TSA and 5AzaC on several predicted REST/NRSF target genes suggests that there will be numerous genes exhibiting REST/NRSF-dependent silencing that require DNA methylation (e.g., *SMARCe*), as well as genes exhibiting HDAC-dependent repression mediated by REST/NRSF [e.g., otoferlin (OTOF)] (*37*). Both genes require REST for their repression, but overexpression of $CoREST_{RID}$ or $MeCP2_{MBD}$ causes derepression of *SMARCe* in Rat-1 cells (Fig. 3A), whereas OTOF is reactivated only in the TSA-challenged Rat-1 cells (Fig. 3A).

The search for REST/NRSF binding sites revealed that many putative REST-regulated genes were tightly clustered. We found several neuronal-specific genes grouped together in the rat genomic interval 3q22-32 where the *NaCh II* gene is mapped. In this interval, the only RE1/NRSE elements identified by informatics were in the promoters of the REST/NRSF-regulated neuronal-specific *NaCh II*, *GAD1*, and *M4* (*38*, *39*). Although eight sodium channel genes are organized in a cluster that mapped to the corresponding chromosome 2 interval in the human genome, current information permits only the *NaCh III* gene to be clearly mapped to the rat chromosome 3q22-32 interval. The *HoxD9* gene mapped to the same interval (3q24-32), and neither *NaCh III* nor *HoxD9* contained REST/NRSF sites. Such grouping of REST-regulated genes at the rat locus 3q22-32 raised the questions of whether CoREST/MeCP2-mediated silencing is imposed on other REST-regulated genes in the interval (such as *GAD1* and *M4*) and whether a similar mode of repression can be extended to genes not harboring REST response elements (such as *NaCh III* and *HoxD9*).

Data from transcriptional expression profiling in Rat-1 cells demonstrated that *NaCh II*, *NaCh III*, *GAD1*, *HoxD9*, *M4*, and *NeuroD1* were not expressed in Rat-1 cells (Fig. 3B), whereas genes 5′ (such as *GpD2* and *GCg*) or 3′ (such as *Cox1* and *PCNA*) to the interval 3q22-32 were highly expressed. Treatment of

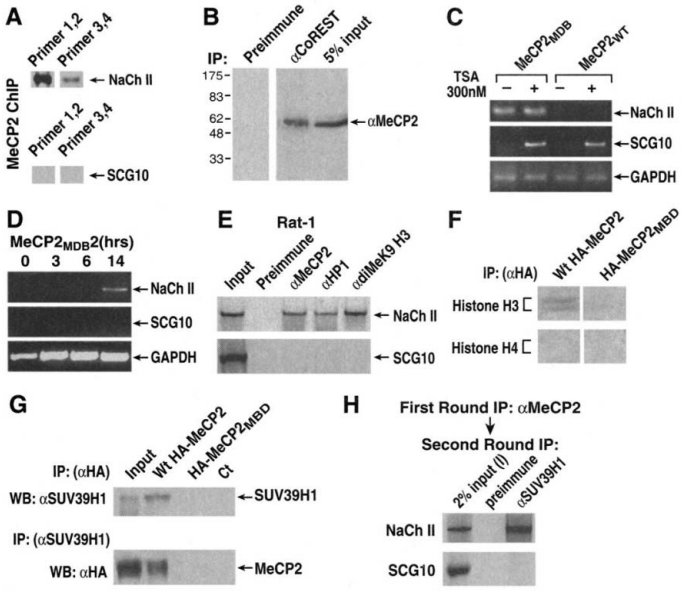

Fig. 2. MeCP2 represses transcription from the endogenous methylated *NaCh II* gene in Rat-1 fibroblasts. (**A**) MeCP2 interacts with the endogenous promoter and 3′ end of the *NaCh II* gene in Rat-1 cells by ChIP analysis. Primers 1 and 2 (promoter) or primers 3 and 4 (coding region) were used for amplification of *NaCh II* and *SCG10* genomic sequences in ChIP analysis. (**B**) MeCP2 complexes with endogenous CoREST protein from Rat-1 nuclear extract (*13*). High-salt nuclear extracts prepared from Rat-1 cells were applied to antibody-agarose containing either preimmune (Preimmune) IgG or affinity-purified antibody to CoREST (αCoREST) and immunoprecipitated material analyzed with the use of antibodies to MeCP2. (**C**) Comparison of derepression of *NaCh II* and sustained repression of *SCG10* genes in Rat-1 cells after transient expression of the methyl DNA-binding domain of MeCP2 ($MeCP2_{MDB}$) and holo-MeCP2 ($MeCP2_{WT}$) in control cells or TSA-treated (for 6 hours) cells. Constitutively expressed *GAPDH* gene was used as a control. (**D**) Time course for derepression of the *NaCh II* gene in Rat-1 cells transiently expressing $MeCP2_{MBD}$. (**E**) A representative ChIP experiment from Rat-1 cells using PCR primers designed for the *NaCh II* and *SCG10* gene promoters with specific antibodies to MeCP2, HP1, dimethyl-K9 H3, or preimmune IgG. (**F**) The MeCP2-associated histone methyltransferases specifically methylate histone H3 (*13*) with the use of equal amounts of transiently expressed HA-tagged wild-type (Wt HA-MeCP2) and mutant (HA-$MeCP2_{MBD}$) MeCP2 in Rat-1 cells. (**G**) SUV39H1 associated with holo-(wtHA-MeCP2) but not the mutant HA-tagged form of MeCP-2 on immunoprecipitation from whole cell extracts with mouse antibodies to HA (*IP:αHA*); Western blots were developed with rabbit IgG to SUV39H1 (αSUV39H1) (top). Extracts precipitated with the use of rabbit IgG to SUV39H1 (IP:αSUV39H1) were analyzed by Western blotting with mouse IgG to HA (αHA) to detect HA-tagged MeCP2. (**H**) Two-stage immunoprecipitation ChIP demonstrated mutual occupancy of the *NaCh II* gene promoter by MeCP2 and SUV39H1 proteins in Rat-1 cells; input from original material.

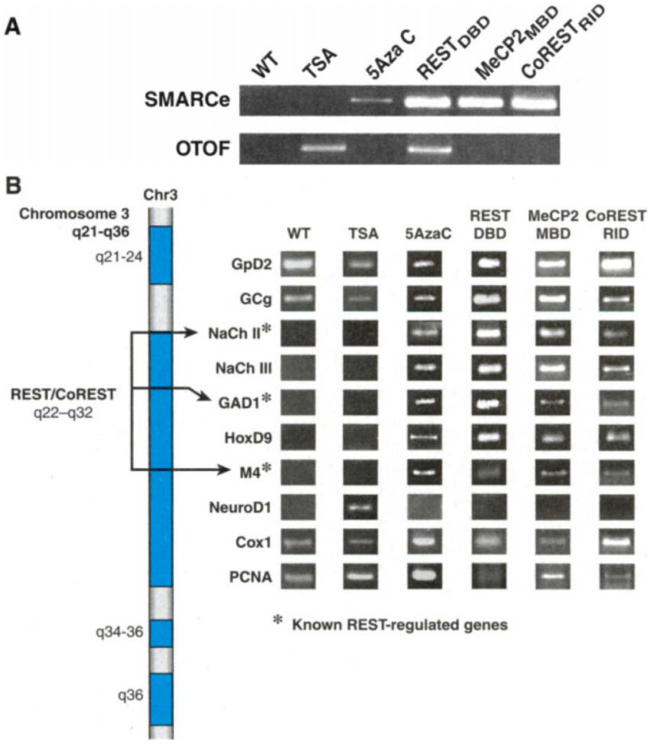

Fig. 3. Chromosomal interval q22-32 on rat chromosome 3 is silenced in a REST/CoREST-dependent manner. (**A**) Analysis of the expression of $SMARC_E$ and *OTOF* genes in Rat-1 cells treated with TSA and 5AzaC, dominant-negative MeCP2, REST/NRSF, or CoREST. (**B**) Derepression of a silent locus on rCh3. Expression profiling for wild-type and TSA- or 5′AzaC-treated Rat-1 cells or Rat-1 cells transiently expressing $REST_{DBD}$, $MeCP2_{MBD}$, and $CoREST_{RID}$ was performed using RT-PCR (one of the experiments shown on the right). Genes containing binding sites for REST/NRSF in their promoters (*NaCh II, GAD1, and M4*) are labeled with an asterisk (*).

Table 1. Representative examples of putative REST/NRSF target genes with a response element adjacent to the promoter based on informatics.

Receptors	
Somatostatin rec 4	(SSTR4)
Seratonin rec 3	(HTR3)
Seratonin rec 6	(HTR6)
Neuronal pentraxin rec	(NPXR)
Histimine rec 3	(HR3)
Dopamine D 3	(DRD3)
GABA rec	(RG2)
Glutamate rec	(GRIK3)
Glutamate rec, kinate2	(GRIK2)
Tyrosin phosphatase rec, typeH	(PTPRH)
Glutamate rec, M4	(GRM4)
Glutamate rec	(GRIK4)
Neurotropic tyrosine kinase rec	(NTRK3)
Glutamate rec	(GRIN2A)
CRH rec 2	(CRHR2)
Growth hormone rel factor rec	(GHRHR)
~Ephrin rec EphA7	(163918)
Amyloid b (A4) PLP1	(APLP1)
Melatonin rec 1B	(MTHR1B)
Olf-rel receptor-4F3	(168119)
~Olf-rel receptor	(123278)
Receptor-associated	
Dvl 1	
G-protein signaling 1	(135997)
Tetraspan TM4SF	(TSPAN-2)
Sweet-taste rec T1R3	(126788)
Ligands/neutrophils	
Urocortin	(UCN)
Neural pentraxin 2	(NTPX2)
Proenkcphalin	(PENK)
Orexin	(HCRT)
Angiogenesis	
ADAMTS2	(Disintegrin)
~ADAMTS-9 (disintegrin)	(125614)
~ADAMTS-9	(160783)
Angiopoietin 4	ANGPT4
Brain-spec angiogenesis inhibitor 2	(BAI2)
Adhesion 1	
Cadherin-like	(CDH22)
~Tubulin b 2 chain	(138099)
Vitronectin	
SYT5	(SYT5)
Myosin VB	MY05B
Teneurin 2	(134424)
~Ankyrin binding protein	(169415)
Neurofilament 3	(NEF3)
Centaurin gamma 1	CENTG1
Enzymes	
Cdk 5 Reg subunit 2	CDK5R2
GAD1	
MGAT3	
MMp24	
Phenylalanine hydroxylase	PAH
PAK7	
Serine protease	P22
Binding proteins	
Oxysterol BP5	OSBP5
Oxysterol BP2 (retina)	OSBP2
Transcription factors/cofactors	
POU5P2	
POU4P3	
Med-6	
DDX30	
RNF30	
Nuclear rec coactivator 5	(NCoA5)
DNA remodeling	
DNMT 3A (embryonic)	(DNMT3A)
•~**SMARCe**	**(130482)**
Nerve terminals/signaling	
Regulator of G-protein 10	(RGS10)
Channels	
Na ChII	
~Voltage gated Na+ channel	(33591)
K+ Ch.NAB2	(KCNAB2)
Hyperpolariz activated Chrom K+	(HCN4)
Ether-a-go-go	
HCN2	
~Ether-a-go-go-like K+ channel	(165681)
Task 3 (K+) channel KCNK9	
Volt depend Ca+ channel	(CANA1H)
Voltage-gated sodium chb-3 sub1	(HSA243396)
KCNJ6	
RNA binding proteins	
Bruno-like 4	(BRUNOL4)
Guidance/migration	
Adhesion/cytoskeletal	
Sema domain/7 thromospondin repeats	(SEMA5A)
Neurofilament 3	(NEF3)
~Ankyrin-like p. 1	(169415)
Complexin 2	(CPLX2)
Carrier/transport	
Sodium CA+ exchanger	(Sic2A8)
ATPase, Cu++ trans, b -subunit	(ATP7B)
~Similar to SNARE Vtilla-b-protein	(143187)
ATPase, Ca++ trans plas membr 2	(ATP2B2)
Putative Na-coupled cotransporter	(RKST1)
Secretion	
CPLX2	
SIC2A8	
AP3B2	
Solute carrier, member 11	(SLC6A11)
Solute carrier family 12	(SLC12A5)
Solute carrier family 6	(SLC6A11)
Solute carrier family 23	(SLC23A1)
Chromagranin B	(CHB B)
Others	
Calneuris	(136832)
Neurexophilin	
NRXN3	
MEGF11	
Cerebellin	(CBLN1)
SPIR2	
~A Rhodopsin 1	(163535)
OSBP2	
~Psoriasin1	(149017)
BCAN	
•**Otoferlin**	**(OTOF)**
CAC RR35	
CARPX	
RES4	
BCAN	
Parvin beta	(PARVB)
Placental	
PP13	
PP13-like	(56891)
PP13-like	(FCGBP)
Ubiquitin-associated 3A	(UBASH3A)

Rat-1 cells with TSA did not alter the basal level of expression of genes within the putative REST/NRSF-dependent gene interval but did cause activation of the *NeuroD1* gene (Fig. 3B and fig. S5). However, we observed a derepression of all tested genes in the interval flanked by the *NaCh II* and *M4* REST/NRSF target genes when treated with 5AzaC (Fig. 3B). Thus, we could suggest that the region 3q22-32 between the *NaCh II* and the *M4* genes is silenced in a DNA methylation–dependent fashion, with the REST-regulated genes potentially serving as organizers of the silent interval. Consistent with this model, *NaCh II*, *NaCh III*, *GAD1*, *HoxD9*, and *M4* were all reactivated by overexpression of the $REST_{DBD}$, $CoREST_{RID}$, or $MeCP2_{MBD}$ dominant-negative factors (Fig. 3B). However, no reactivation of the transcriptional activity of another repressed gene, *Neuro D*, was observed in the same experiments.

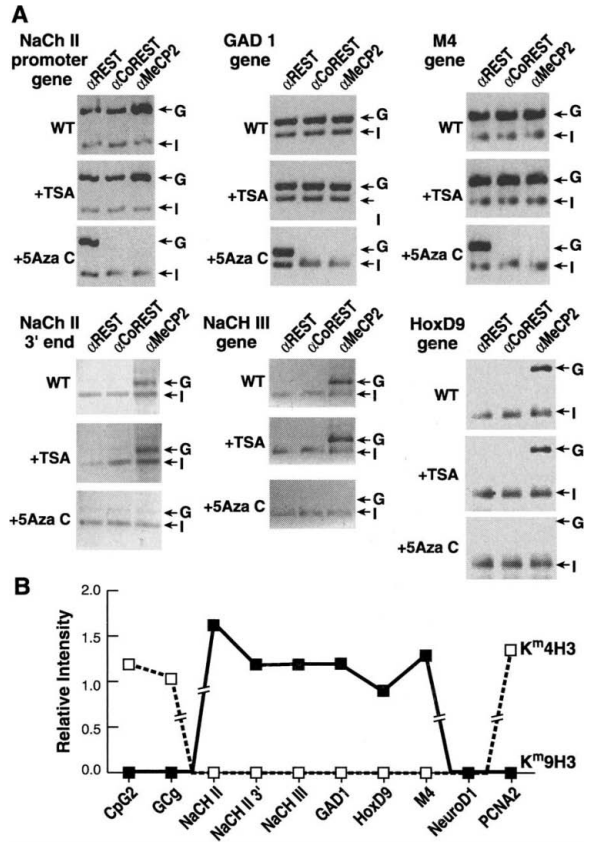

Fig. 4. REST, CoREST, and MeCP2 proteins associate with the 3q22-32 genomic interval. (**A**) The endogenous promoters *NaCh II*, *NaChIII*, *GAD1*, *M4*, *HoxD9*, and a 3′ coding region of *NaCh II* genes were analyzed by ChIP. Experiments were performed in wild-type Rat-1 cells and Rat-1 cells challenged by TSA or 5AzaC treatment. Positions of PCR products obtained by the amplification of genomic segment (G) and internal standards (I) are indicated. (**B**) Chromosomal region 3q22-32 reveals specific H3 modification at Lys^9 ($\alpha K^m 9H3$). ChIP experiments were performed with antibodies to dimethyl-K9 H3 and dimethyl-K4 H3 across and outside of the silent interval.

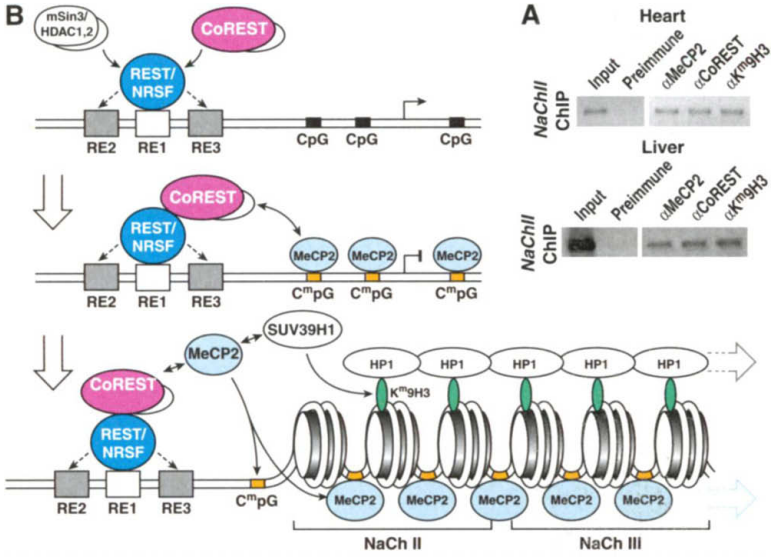

Fig. 5. CoREST-dependent gene silencing. (**A**) ChIP analysis of the *NaCh II* promoter in vivo, using murine liver and heart tissues and antibodies specific to CoREST, MeCP2, and K^m 9H3. (**B**) Model of REST/CoREST-dependent silencing of a chromosomal interval, showing that binding of REST and specific CpG methylation events permit recruitment of CoREST and subsequent assembly and spreading of silencing machinery.

The results indicated that REST/NRSF and CoREST were associated only with the promoters of REST/NRSF-regulated genes (*NaCh II, Gad1, M4*) and not detected on the 3′ end of *NaCh II* gene or on the promoters of *NaCh III* or *HoxD9* genes (Fig. 4A). This is consistent with predictions of the informatics search. In contrast, MeCP2 was present throughout the interval on the six tested genomic segments. Thus, although treatment with TSA did not substantially reduce the degree of MeCP2 occupancy on promoters of these genes, the genomic demethylation consequent to 5AzaC treatment was associated with release of MeCP2 from all of the segments within the interval (Fig. 4A).

Whereas REST/NRSF association with promoters of these genes was observed regardless of methylation status (Fig. 4A), CpG methylation appeared to be required for REST/NRSF/CoREST complex formation on the promoters of *NaCh II*, *GAD1*, and *M4* genes, because binding of CoREST was eliminated after treatment with 5AzaC (Figs. 4A and fig. S5). Treatment with TSA had no functional effect on the repression status of the genes in the interval (Fig. 3B) and did not alter the associations of CoREST and MeCP2 proteins with tested genes (Figs. 3B and 4A).

These data are consistent with a model whereby the presence of a REST-CoREST complex on specific promoters nucleates a progressive silencing across the interval, perhaps by sequestering the methylation-modified chromatin to an inactive nuclear matrix to allow silencing to spread across the interval. Because the "histone code" serves critical epigenetic aspects of transcriptional control and the correlation of specific histone H3 modifications in silencing of the globin locus, X chromosome inactivation, and the MHL loci in yeast (*23*, *27*, *32*), we were particularly interested in evaluating the presence of K^m9 histone H3 and K^m4 histone H3 across the interval by ChIP analysis, with internal standard segments. All known gene targets in the rat Ch3 p22-32 interval contained dimethyl K9 histone H3 but not methyl K4 histone H3 (Fig. 4B and fig. S6). This correlation is similar to that observed for the silenced β globin locus (*33*).

Corepressor-dependent silencing by REST/NRSF. We conclude that the zinc-finger factor REST/NRSF can mediate both ac-

tive repression via recruitment of specific HDACs and gene silencing by recruitment of CoREST complexes (*10–12*) to specific promoters in a cell type– and promoter-specific DNA methylation manner.

Similar events occur in vivo, with CoREST, MeCP2, and $K^{m}9H3$ markers of silencing proving to be present on the *NaCh II* promoter in adult murine liver and heart (Fig. 5A). With the use of MEME and SP-STAR motif–finding algorithms (*38*), we located two motifs that are present preferentially within 250 bp of an experimentally confirmed RE1/NRSE consensus site that may be related to the known RE1/NRSE consensus site (fig. S7). The full importance of these motifs will need to be genetically studied, but one (RE2) is capable of both transcriptional repression and REST/NRSF binding (*14*). Thus, analogous to nucleation of gene silencing at specific sequences [polycomb group response elements (PREs)] (2), we suggest that the RE1/NRSE element, perhaps in concert with related sites, might nucleate silencing of specific chromosomal regions.

Recruitment of the corepressor CoREST to REST/NRSE gene targets appears to act as a molecular beacon for the silencing machinery, including MeCP2, SUV39H1, and HP1, to propagate and maintain a methyl CpG-dependent silent state across specific chromosomal intervals, including genes that do not contain REST/NRSF-binding sites (Fig. 5B). This model is consistent with observations that DNA methylation by itself is not sufficient for silencing (*41*). MeCP2 appears to be a critical component of these events in Rat-1 cells, but other factors may operate in cell types where MeCP2 is not expressed. The recruitment of SUV39H1, in part via interactions with MeCP2 complexes, apparently leads to HP1 recruitment and chromatin condensation in cultured cells and in vivo (Fig. 5B). The presence of $K^{m}9$ but not $K^{m}4$ histone H3 across the rCh3 q22-34 region is consistent with CoREST-mediated recruitment of silencing machinery and the proposed epigenetic program (*27*, *28*, *31*, *35*, *39*).

These observations further suggest that other factors analogous to REST are likely to mediate the silencing of distinct chromosomal regions that regulate other biological programs, some via recruitment of CoREST complexes. Conversely, the expression of REST/NRSF early in brain development and the potential silencing of genes such as $SMARC_E$ suggest that REST/NRSF may also control important roles in early embryonic gene silencing.

References and Notes

1. E. J. Richards, S. C. Elgin, *Cell* **108**, 489 (2002).
2. C. J. Schoenherr, D. Anderson, *Science* **267**, 1360 (1995).
3. J. A. Chong *et al.*, *Cell* **80**, 949 (1995).
4. C. J. Schoenherr, A. J. Paquette, D. J. Anderson, *Proc. Natl. Acad. Sci. U.S.A.* **93**, 988 (1996).
5. N. Mori, R. Stein, D. Sigmund, D. J. Anderson, *Neuron* **4**, 583 (1990).
6. N. Ballas *et al.*, *Neuron* **31**, 353 (2001).
7. Y. Naruse, T. Aoki, T. Kojima, N. Mori, *Proc. Natl. Acad. Sci. U.S.A.* **96**, 13691 (1999).
8. K. Jepsen *et al.*, *Cell* **102**, 753 (2000).
9. M. E. Andres *et al.*, *Neuron* **96**, 9873 (1999).
10. A. You, J. K. Tong, C. M. Grozinger, S. L. Schreiber, *Proc. Natl. Acad. Sci. U.S.A.* **98**, 1454 (2001).
11. G. W. Humphrey *et al.*, *J. Biol. Chem.* **276**, 6817 (2001).
12. M. A. Hakimi *et al.*, *Proc. Natl. Acad. Sci. U.S.A.* **99**, 7420 (2002).
13. Materials and methods are available as supporting material at *Science* Online.
14. V. V. Lunyak *et al.*, unpublished data.
15. A. Razin, M. Szyf, *Biochim. Biophys. Acta* **782**, 331 (1989).
16. S. Tweedie, S. Charlton, V. Clark, A. Bird, *Mol. Cell. Biol.* **17**, 1469 (1997).
17. M. Brandies, M. Ariel, H. Cedar, *Bioassays* **15**, 709 (1993).
18. P. H. Tate, A. Bird., *Curr. Opin. Genet. Dev.* **3**, 226 (1993).
19. Z. Siegfried, S. Eden, M. Mendelsohn, X. Feng, B. Z. Tsuberi, H. Cedar, *Nature Genet.* **22**, 203 (1999).
20. J. D. Lewis *et al.*, *Cell* **69**, 905 (1992).
21. M. C. Lorincz, D. Schubeler, M. Groudine, *Mol. Cell. Biol.* **21**, 7913 (2001).
22. R. E. Amir *et al.*, *Nature Genet.* **23**, 185 (1999).
23. R. X. Chen, S. Akbarian, M. Tudor, R. Jaenisch, *Nature Genet.* **27**, 327 (2001).
24. A. C. Bell, G. Felsenfeld, *Nature* **405**, 482 (2000).
25. K. Kokura *et al.*, *J. Biol. Chem.* **276**, 34115 (2001).
26. R. I. Gregory *et al.*, *Mol. Cell. Biol.* **21**, 5426 (2001).
27. E. Heard *et al.*, *Cell* **107**, 727 (2001).
28. S. Rea *et al.*, *Nature* **406**, 593 (2000).
29. K. Mechtler, C. P. Ponting, C. D. Allis, T. Jenuwein, *Nature* **406**, 593 (2000).
30. J. C. Rice, C. D. Allis, *Curr. Opin. Cell Biol.* **13**, 263 (2001).
31. K. Noma, C. D. Allis, S. I. Grewal, *Science* **293**, 1150 (2001).
32. A. J. Bannister *et al.*, *Nature* **410**, 120 (2001).
33. M. D. Litt, M. Simpson, M. Gaszner, C. D. Allis, G. Felsenfeld, *Science* **293**, 2453 (2001).
34. M. Lachner, D. O'Carroll, S. Rea, K. Mechtler, T. Jenuwein, *Nature* **410**,116 (2001).
35. J. Nakayama, A. J. Klar, S. I. Grewal, *Cell* **101**, 307 (2000).
36. J. Nakayama, J. C. Rice, B. D. Strahl, C. D. Allis, S. I. Grewal, *Science* **292**, 10 (2001).
37. P. A. Pevzner, S. H. Sze, *Intelligent Systems in Molecular Biology* (AAAI Press, La Jolla, CA, 2000), pp. 269–278.
38. M. Mieda, T. Haga, D. W. Saffeen, *J. Biol. Chem.* **272**, 5854 (1997).
39. I. C. Wood, A. Roopra, N. J. Buckley, *J. Biol. Chem.* **271**, 14221 (1996).
40. T. Jenuwein, C. D. Allis, *Science* **293**, 1074 (2001).
41. P. Jones, *Nature Rev. Genet.* **3**, 415 (2002).

42. We particularly thank A. Gonzalez (Santa Cruz Biotech Inc.) for helpful advice, K. Ohgi for technical assistance, and P. Myer and M. Fisher for figure and manuscript preparation. M.G.R. is an Investigator and V.L. is an Associate with HHMI. G.P. is supported by the Canadian Institute of Health Research. Supported by grants from NIH to G.M. and M.G.R. and a grant from CapCURE to M.G.R.

Supporting Online Material

www.sciencemag.org/cgi/content/full/1076469/DC1
Materials and Methods
Figs. S1 to S7

23 July 2002; accepted 23 September 2002
Published online 24 October 2002;
10.1126/science.1076469
Include this information when citing this paper.

Martian Meteorite Launch: High-Speed Ejecta from Small Craters

James N. Head,[1,2] H. Jay Melosh,[1] Boris A. Ivanov[3]

We performed high-resolution computer simulations of impacts into homogeneous and layered martian terrain analogs to try to account for the ages and characteristics of the martian meteorite collection found on Earth. We found that craters as small as ~3 kilometers can eject $\sim 10^7$ decimeter-sized fragments from Mars, which is enough to expect those fragments to appear in the terrestrial collection. This minimum crater diameter is at least four times smaller than previous estimates and depends on the physical composition of the target material. Terrain covered by a weak layer such as an impact-generated regolith requires larger, therefore rarer, impacts to eject meteorites. Because older terrain is more likely to be mantled with such material, we estimate that the martian meteorites will be biased toward younger ages, which is consistent with the meteorite collection.

Past models of the origin of the martian meteorite suite (*1–3*), which supposed that the meteorites were launched from relatively large craters, are unable to account for the presently known distribution of cosmic ray exposure (CRE) ages (*4*). Using the known present-day lunar flux of impactors, extrapolated to Mars (*5*, *6*), the probability of even one 12-km-diameter crater forming on Shergottite-age terrain is ~0.04. In contrast, CRE ages (Table 1) and petrology (*7*, *8*) indicate that the known martian meteorites were launched in six or seven events. Thus, the observed launch frequency disagrees by two orders of magnitude with the estimated cratering rate. Appeals to statistics of small numbers are unsatisfactory, given the large number of launch events now recognized.

[1]Department of Planetary Sciences, University of Arizona, 1629 East University Boulevard, Tucson, AZ 85721, USA. [2]Raytheon Missile Systems, Post Office Box 11337, Building 805, M/S L5, Tucson, AZ 85734–1337, USA. [3]Institute for the Dynamics of Geospheres, Russian Academy of Sciences, Moscow, Russia 117939.